Predator and prey encounter rates and local prey densities are modulated by prey behavior

Matthew S. Woodstock[1,*], Jann Paul Mattern[2], Gregory L. Britten[1]

[1]Woods Hole Oceanographic Institution, 266 Woods Hole Road, Woods Hole, MA, 02543, USA

[2]Department of Ocean Sciences, University of California Santa Cruz, 1156 High St., Santa Cruz, 95064, USA

[*]Corresponding Author: Matthew S. Woodstock (matthew.woodstock@whoi.edu)

Abstract

The predation efficiency of an animal is a function of the surrounding prey density but is also influenced by various ecological and ethological factors that cause limitations to the foraging capacity of the predator. Food-web models rely on predation efficiency estimates to calculate consumption rates, but these models often lack the resolution to consider predators as individual entities with different predation success rates. Individual-based modeling can provide this resolution and is becoming more tenable as computational power increases. We developed a three-dimensional, two-species model that includes varying predator and prey swimming velocities, visual abilities, and a range of prey abundances to evaluate the effect on encounter rates, functional response curves, and estimated consumption rates. Encounter rates were a function of prey abundance, following a Type II ecological functional response curve (logarithmic curve) for all simulations where the predator was at least twice as fast as the prey. The effective attack rate of the predator was influenced by the relative swimming velocity between predator and prey, and partially by the prey's visual ability, affecting the steepness and asymptote of the functional response curve. Although each predator could perceive 50% of the model domain volume, the number of preys within each predator's visual range (i.e., local prey density) was almost always less than 50% in all simulations, indicating that the emergent prey

field was heterogeneous. The emergent consumption rate estimates from local prey densities were less than global prey densities, and local prey densities had variance scaled to the variability in local prey densities among all predators. Local prey densities are a necessary calculation for individual-based predator/prey models because they provide refined consumption rate estimates based the immediate surrounding prey field with considerations to behavioral impacts that modulate predator/prey dynamics.

Keywords: Predator/prey dynamics, Individual-based modeling, Food webs, Functional Responses, Theoretical Modeling, Agent-based modeling

Introduction

The foraging efficiency of a predator is a density-dependent, hyperbolic function of the surrounding prey density, handling time, digestion rates, and satiation of the predator, which influence encounter rates (Jeschke et al. 2002, Li et al. 2018, Papanikolaou et al. 2020). Changes to prey density results in a non-additive adjustment to a predator's estimated consumption rate, commonly termed ecological functional response curves (Holling 1965). Several variations of these functional response curves provide a more refined estimation of predator foraging rates, with variations according to food-web complexity (Chan et al. 2017), predator density (Cosner et al. 1999, Kratina et al. 2009), and habitat complexity (Grabowski 2004), among others. Moreover, animals alter their behavior when presented with potential threats in ways that affect predator-prey encounter rates, predator consumption effects, and energy landscapes in marine ecosystems (Preisser et al. 2005, Papastamatiou et al. 2023). Animals attempt to avoid these threats in an environment where the predator has an alternative goal of increasing predation success. The relative sensory capabilities (e.g., vision) that allow both predator and prey to perceive their environment and the swimming velocities will likely determine the influence of these behaviors on encounter rates. Swimming velocities roughly correspond to their body shape,

body size, and additional characteristics (e.g., scombrid keels), which affect the animal's ability to reduce drag and produce thrust in a viscous medium (Liao 2007). A prey's ability to both perceive and avoid predators could lead to reduced encounter rates compared to preys that cannot avoid predation, resulting in a dampened functional response curve and reduction in the theoretical foraging efficiency of a predator.

Despite the explored variations in functional responses, many popular food-web models are not capable of simulating populations at the individual scale, and thus cannot incorporate individual-based factors that influence functional response curves. Instead, simplistic versions of functional response curves are utilized, largely making these assumptions based on static (i.e., not changing after calibration) state parameters and spatiotemporally dynamic prey densities. Agent-based models (i.e., individual-based models) are capable of simulating populations at the individual scale and explicitly modeling informed animal decisions (Thiele et al. 2011). However, their utilization into complex ecological modeling techniques has been limited by the computational expense of explicitly modeling individuals at large, but fine spatiotemporal scales. This computational limitation leads to the aggregation variables that are less important to the central model question (Plagányi et al. 2014), which could be sufficient in certain situations. However, there is strong logic behind incorporating species' traits in ecosystem-scale modelling efforts (Weisberg et al. 2023), which will require refined individual-scale modeling approaches. Novel food-web modeling and ecological network analysis methodologies are being developed with faster programming speeds using the Julia Programming Language (Banville et al. 2021), creating the possibility for individual-based modeling at fine spatiotemporal scales (Wu and Forget 2022). The application of an individual-based model as an ecosystem-scale food-web

model requires a mechanistic understanding of how individual animal decisions may influence a predator's foraging efficiency and subsequent consumption rates.

Marine populations are often organized as heterogenous patches, were individuals are tightly aggregated in one location at a higher density than a background density (Levin 1994). This patchiness influences future animal movements as predators perceive prey patches and orient themselves within areas of high prey density, ostensibly to increase foraging success (Kacelnik et al. 1992). Since predator-prey encounter rates are related to prey densities, each predator individual could experience different prey densities, and subsequent estimated encounter rates. However, food-web models are often applied at singular spatial scales (i.e., the same spatial scale for each species/functional group) and that spatial scale may be coarser than an individual predator could perceive within a defined temporal scale. This mismatch limits the model's ability to simulate the patchiness that may emerge from fluid dynamics and active animal movements. A more accurate estimate may be to calculate the number of preys in the perceivable area of each predator and calculate individual predator foraging efficiencies (Figure 1). These individual calculations, and the processes that determine differences among predator individuals, can only be simulated using an individual-based model.

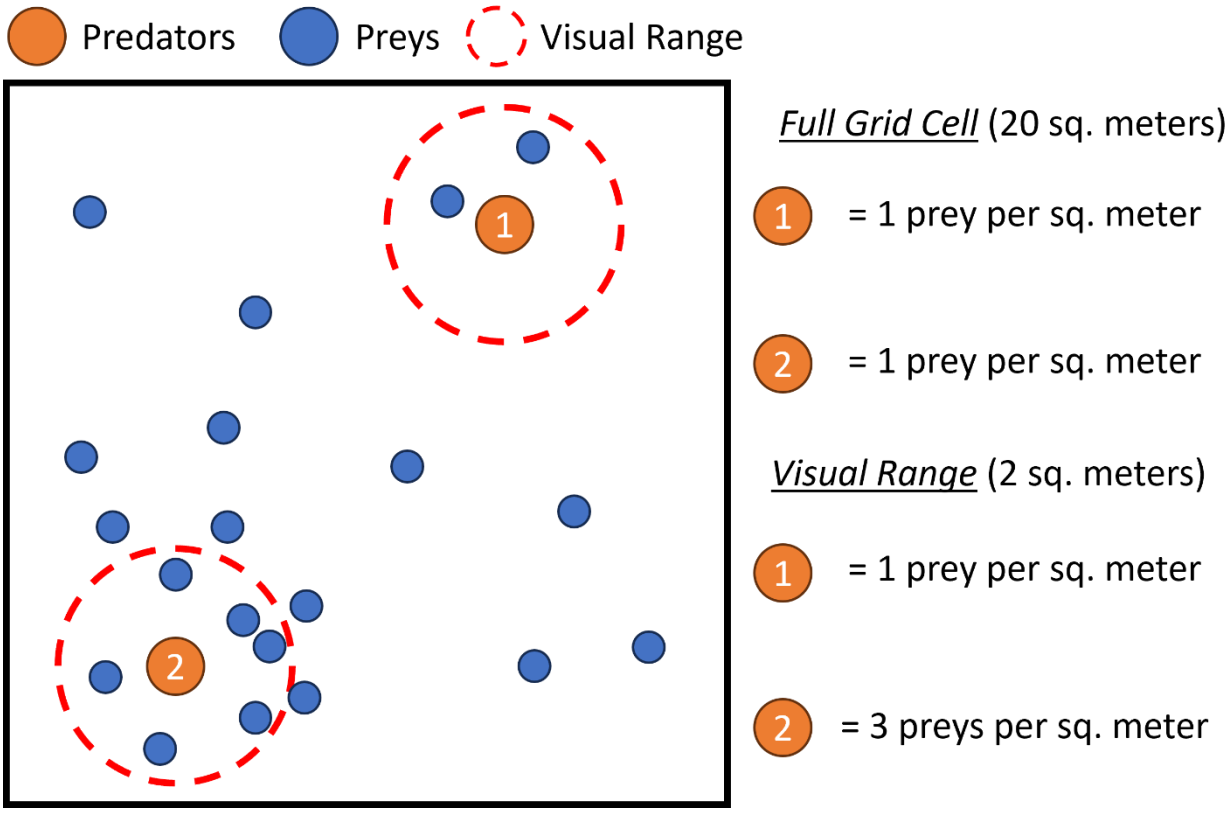

Figure 1. A schematic of the challenges associated with calculating prey density in an individual-based framework as two predators (orange) have different prey (blue) densities depending on if that density is calculated from the global scale (full grid cell) or localized scale (the visual range of the predator; red). The perception range could apply to all sensory functions.

In this study, we developed a three-dimensional, two-species model to examine changes in the encounter rates of predators and preys among a range of prey abundances, swimming velocities, and visual ranges. Functional response curves emerged as the relationship between encounter rates in the simulation and a progression of examined prey abundances. The effect of prey swimming velocities and visual ranges were tested and described in relation to the predator swimming velocity and visual range and this effect was integrated into a novel ecological functional response curve equation. Predator-specific prey densities were calculated as both a grid-based density and individual-based density and consumption rate estimates were derived.

Methods

Model Structure

The encounter rates of predator and prey species were examined using a modified version of *PlanktonIndividuals.jl* (Wu et al. 2022) that allowed for direct and active animal movement, and limitations to an animal's perception of its environment (i.e., visual range, hereafter). The theoretical model domain was a 100 meters x 100 meters x 100 meters cube (1,000,000 cubic meters in volume) with no structural habitat, best simulating a pelagic environment. Only active movement (i.e., swimming) was considered and no spatial restrictions were placed on animal movement (i.e., the entire habitat was considered equally suitable). Both the predator and prey species were provided with a scalar movement velocity vector during each simulation (Table 1).

Table 1. The state variables used during the simulation and the calculation of consumption perceivable prey density

Parameter	Value	Units
Simulation Parameters		
Predator Abundance	100	Individuals
Prey Abundance	25–900	Individuals
Predator Swim Speed	0.01	$m\ s^{-1}$
Prey Swim Speed	0.0001–1	$m\ s^{-1}$
Predator Visual Range	49.2	m
Prey Visual Range	0–62.04	m
Simulation Length	300	minutes
Handling Time	8	minutes
Consumption Parameters		
Prey Weight	5	g
Prey Energy Density	5,000	Joules
Predator Capture Success	0.7	Dimensionless

Simulations

The predator-prey encounter rates were examined as a function of prey abundance (25–900 individuals at varying intervals), prey velocity (0.0001–1 $m\ s^{-1}$), and prey visual field (0–62.04 m radius; Table 1). Predator velocity (0.01 $m\ s^{-1}$), predator visual field (49.2 m radius; i.e., half of the model domain volume), predator abundance (n = 100 individuals), and predator handling

time (8 minutes) were the same in each simulation. In this study, the handling time parameter is considered to also include digestion time. Boundary effects (i.e., preys trapped in model domain corners by predators) were removed by allowing both predators and preys to "jump" from one end of the grid to another, creating an endless domain. The domain size, movement velocities, and visual fields were chosen to provide a relative representation of two hypothetical species. Since these parameters will vary with species' morphology and visual capabilities, these parameters do not necessary represent a particular predator-prey interaction, but instead are designed to explore how encounter rates vary with respect to relative differences in predator/prey characteristics. Prey abundances remained constant throughout each simulation (i.e., no fluctuation prey abundance) and consumed preys were respawned at random coordinates. Random spawning potentially created encounters if a prey was spawned in a suboptimal location near a predator, so ten iterations were conducted for each scenario. All predators and preys moved at each time step. The predators attempted to move towards the closest prey and the prey attempted to move towards the optimal location to avoid all predators within their visual range (i.e., furthest location from all predators). If there were no preys within the predator's visual range or no predators within the prey's visual range, the individual moved at a random vector at a distance consistent with their swimming velocity. When predators reached preys, consumption occurred, and an eight-minute handling time period was applied to that predator. The simulation continued for 300 minutes at a one-minute scale. The encounter rate (N encounters $timestep^{-1}$) was calculated for each simulation and comparisons were made among prey velocities, visual fields, and abundances.

The modeled prey abundances (P), handling time (h), and emergent encounter rates (enc) were utilized to estimate the optimal effective attack rate (a) for each prey swimming velocity

and visual range pair (Equation 1). The optimization was completed using the R programming language and the *optim()* function in the "stats" package (R Core Team 2023) with a starting *a* value of 0.01 and potential range of 0–5000. All iterations were able to converge, but simulations with a RMSE greater than 5 were removed, as they did not follow the appropriate Type II functional response curve. All the removed functional response curves had less than 0.01 encounters timestep^{-1}, regardless of the modeled prey abundance. The estimated effective attack rates were compared among prey swimming velocities and visual ranges.

$$enc_{vis,velo} = \frac{a_{vis,velo} P_{vis,velo}}{1 + a_{vis,velo} h P_{vis,velo}} \quad (1)$$

Two prey densities were calculated during each simulation, a global prey density (prey abundance / volume of model domain) and local prey density (n perceivable preys / volume of perceivable area). Within simulations, the global prey density was the same for each predator because prey abundance and the size of the model domain were constant throughout the simulation. However, each predator could experience a different local prey density and this value could vary throughout the simulation for each individual. The number of preys within each predator's perceivable area was recorded during the last timestep of each simulation. The last timestep reflected the combined effects of each preceding timestep's animal movements and had the most refined estimate of the preys surrounding each predator. Global and local prey densities were converted to consumption (*C*; Joules) according to an assumed Type II ecological functional response curve (Equation 2).

$$C_{vis,velo} = p_c * w * d * enc_{vis,velo} \quad (2)$$

where the encounter rate is derived from equation 1 with the newly acquired local prey densities, estimated attack rate, and same handing time parameter. A predator success coefficient (p_c; 0.7),

prey weight (*w*; 5 g), and prey energy density (*d*; 5,000 J) convert the estimated encounter rate to the possible biomass consumed during that time step. Although the initial model assumed predators were always successful, a value of 0.7 was considered more realistic and was applied to both grid-based and individual-based densities. The chosen values represented those that may be realistic for this model domain, but could be any, as they scale equally for both global and local prey density-consumption calculations.

Results

Encounter Rates

The encounter rates experienced between predator and prey were a function of prey density and followed a Type II ecological functional response curve (Figure 2). Encounter rates were smallest at the smallest prey abundance (n = 25 preys), ranging from 5×10^{-3} ($\pm 3 \times 10^{-3}$) encounters timestep^{-1} at the fastest simulated prey velocity to 0.44 ($\pm$0.02) encounters timestep^{-1} at the slowest simulated prey velocity. Encounter rates were greater when preys were blind (0 m prey visual range) compared to simulations of the same prey velocity and abundance (Figure 2), indicating that the ability for the prey to make optimal movement choices influences ecological functional response curves. When the prey had a visual range greater than 0 m, preys that had an equivalent swimming velocity to the predator always had visual encounter rates less than 0.11 encounters timestep^{-1}, regardless of prey abundance. Beyond the 3 m visual range, the prey's visual acuity had little effect on the predator/prey encounter rate (Figure 2). Prey density and prey velocity have the greatest effect on the encounter rates between predator and prey in a fixed-space ecosystem, while a prey's ability to perceive the environment has limited influence on encounter rates.

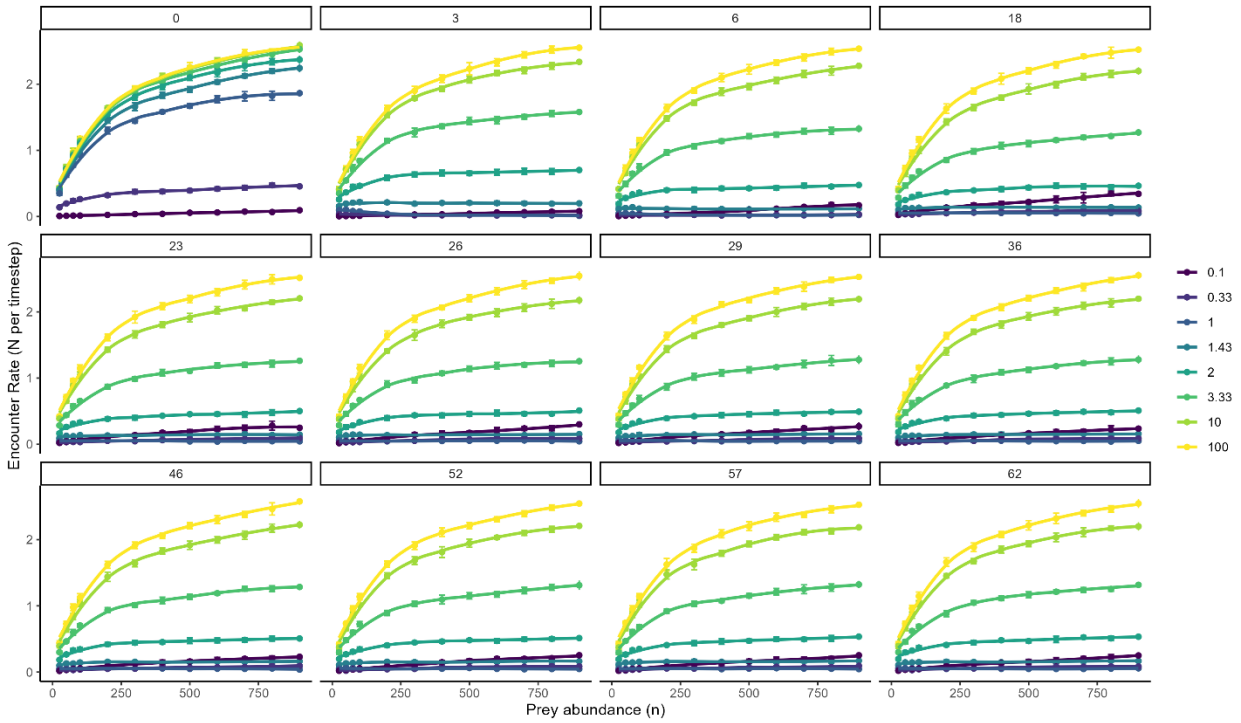

Figure 2. The effects of prey velocity (colors) and visual range (panels) on functional response curves. Visual range panels correspond to the distance the prey can perceive and was calculated as the radius of an assigned visual field volume. The predator velocity (0.01 m s^{-1}), visual range (49 m; half of the model domain), and abundance (n = 100 individuals) were the same in each simulation.

Predator/prey encounter rates have a logarithmic relationship with the relative swimming velocities of predator and prey. When predators are 100x faster than preys, encounter rates have a maximum of 2.6 (± 0.06) encounters $timestep^{-1}$, whereas when preys are 10x faster than predators encounter rates have a maximum of 0.3 (± 0.04) encounters $timestep^{-1}$ (Figure 3). The encounter rates when preys are 10x faster than the predator are similar to simulations where the preys have the same swimming velocity to the predator, when preys are capable of seeing predators. An inflection point occurs in this relationship between equivalent predator/prey swimming velocities and predator velocities greater than 10x the prey (Figure 3). At low predator/prey swim speed ratios, prey abundance does not influence the number of encounter

rates. However, at high predator/prey swimming speed ratios, the highest prey abundances also influence prey encounter rates. Encounter rates are influenced by the prey's ability to avoid predation, and this effect is greatest in between equivalent predator/prey swimming velocities and when predators are one order of magnitude faster than preys.

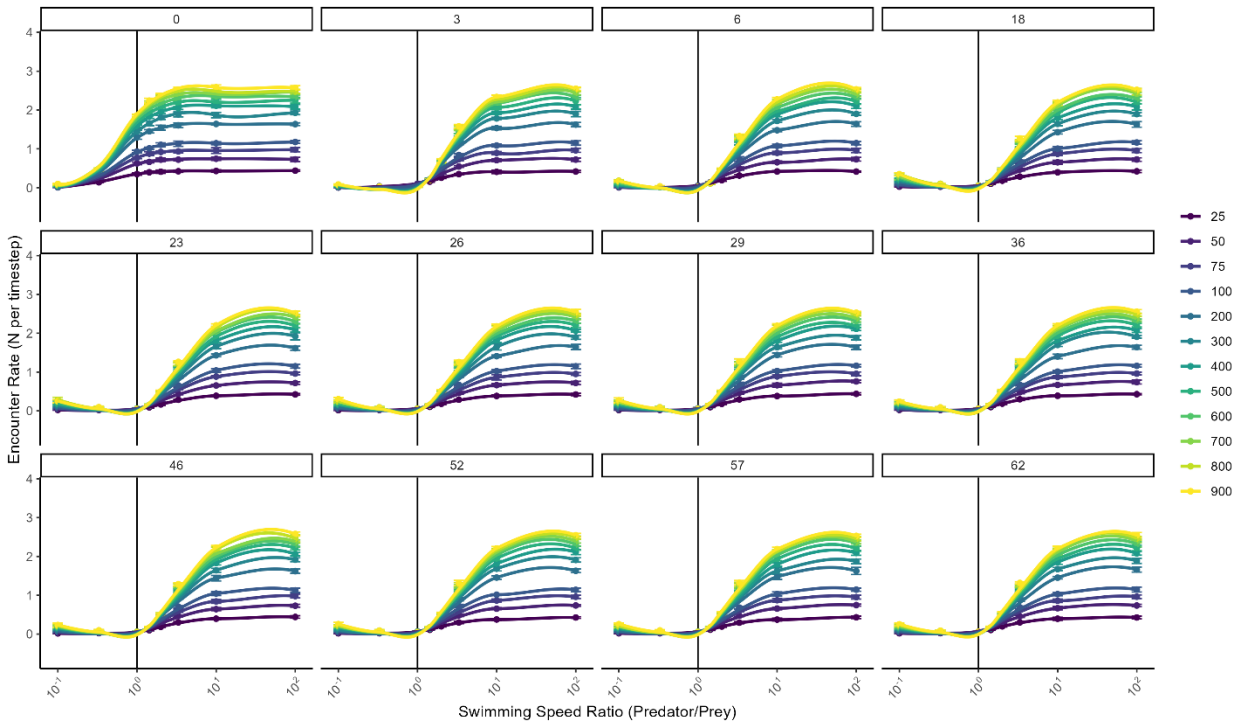

Figure 3. The relationship between predator-prey encounter rates and predator-prey relative swimming velocities (log-transformed). Prey abundances are represented as colors and prey visual range (visual distance; m) are represented as facets. Predator velocity (0.01 m s^{-1}; vertical black line), abundance (n = 100 individuals), and visual range (49 m; half of model domain) are constant in each simulation.

New FR Curve Equation

The relative swimming velocity between predator and prey and visual range had an influence on the attack rate coefficient (*a*) of the functional response curve (Table 2). Preys that were 10x faster than their predator did not align with a Type II functional response curve because they could effectively avoid most encounters at all prey abundances. Preys that could see greater than 3 m or further had similar attack rate coefficients when compared to simulations of the same swimming velocity and only followed a Type II response curve if the predator was at least twice

as fast as the prey. Preys that could perceive their environment had a smaller attack rate coefficient than blind preys for swimming velocity ratios between 2:1–10:1 (Table 2). There was a 6-fold difference in the attack rate for swimming ratios of 100:1 and 2:1 (Table 2). Blind preys were less successful than visual preys at modulating predator attack rates (Table 2). Differing predator attack rates among varying prey swim velocities indicate that the estimated individual-based consumption rate will be different based on the prey's ability to avoid predation.

Table 2. The effective attack rate coefficients (a) for a Type II functional response curve that correspond to the encounter rates. All preys that could see (Visual distance greater than 0) had the same attack rate coefficients. Only pairs that had converged effective attack rate values are reported

Relative Swim Speed	**Blind**	**Not Blind**
0.1	-	-
0.3	0.001	-
1.0	0.004	-
1.4	0.005	-
2.0	0.005	0.001
3.3	0.006	0.003
10.0	0.006	0.005
100.0	0.006	0.006

Prey Density and Consumption

The number of perceivable preys per predator was greatest at high prey densities than at low prey densities for all prey swimming velocity and prey visual range combinations (Figure 4A; Supplemental Figures 1–12). In a homogenous environment where the predator can perceive 50% of the volume, it would be expected that the predator could perceive 50% of all available preys. However, the proportion of all preys within the perceivable area peaked between 20% and 40% per predator among all the prey abundance scenarios, independent of overall prey abundance (Figure 4B). There is a positive relationship between prey density and the variance in the number of perceivable preys per predator (Figure 4C). Since local prey densities were almost always less than 50% of the total available preys, the estimated encounter and consumption rates

that emerge from these prey densities, are anticipated to be less than those derived from a global prey density calculation.

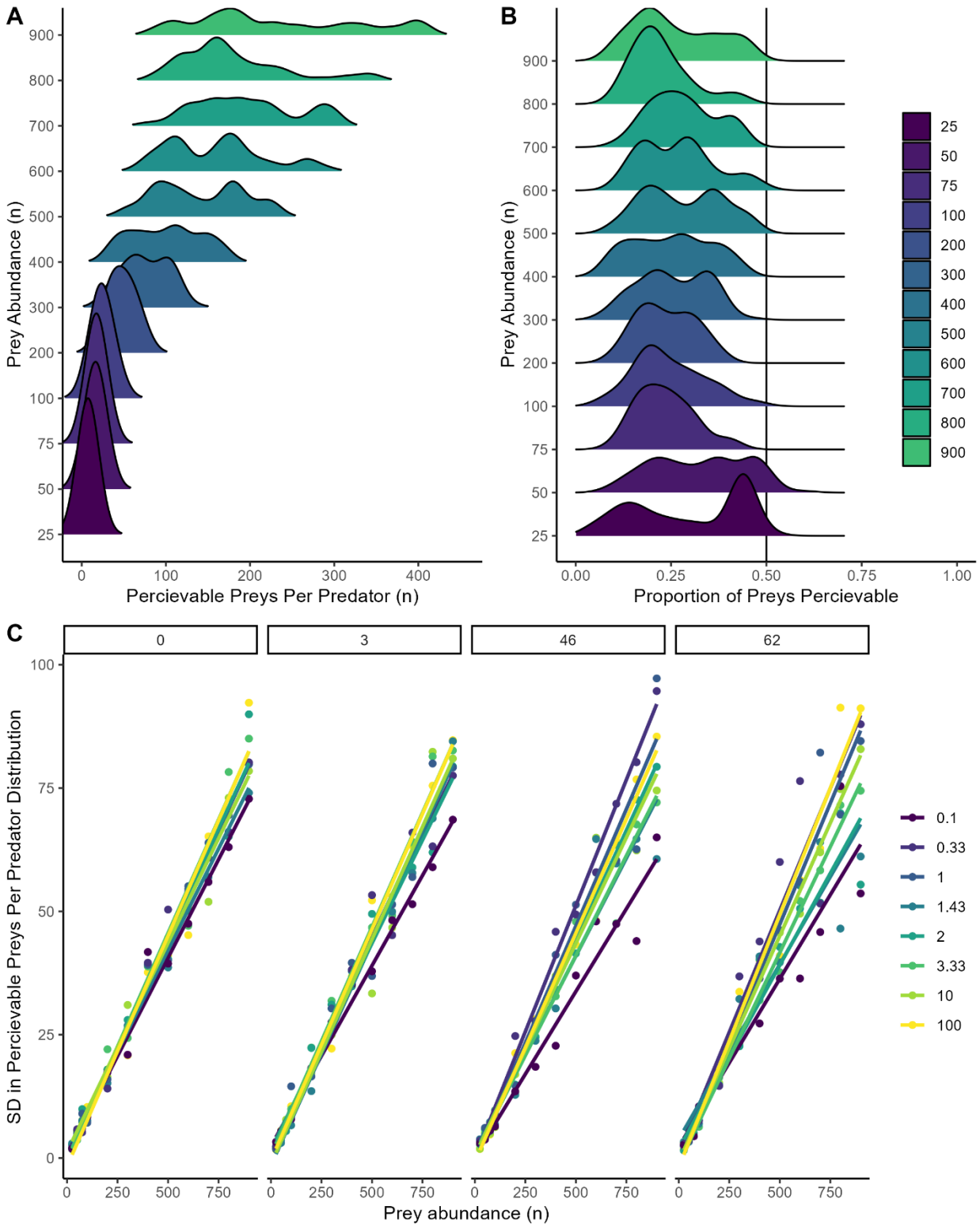

240

241 Figure 4. Ridgeline plots of A) the number of preys within each predator's perceivable area B)
242 and the proportion of available preys within the model domain that were within the perceivable
243 range of the predator. These results only reflect the scenarios where prey velocity was equivalent

to the predator and visual range was 46 m. C) The relationship between the standard deviation of the perceivable prey distribution and modelled prey abundance separated by prey swimming velocity (colors) and prey visual range (facets). Only four select prey visual distances are represented. All other relationships are in Supplemental Figures 1-12.

The emergent effective attack rates and prey densities resulted in global density consumption rate estimates (C_{global}) and local density consumption rate estimates (C_{local}) that varied among prey swimming velocities and visual ranges (Figure 5). The largest effective attack rate (0.006; Table 2) led to the highest asymptote in the C_{global} curve (26.3 J timestep^{-1} predator^{-1}; Figure 5), while the lowest effective attack rate (0.001; Table 2) resulted in the lowest asymptote of the C_{global} calculation (8.0 J timestep^{-1} predator^{-1}; Figure 5). Since the C_{global} calculation involved two constants (number of preys within the model domain, model domain volume), there was no within-simulation variance in this curve. The C_{local} estimates were consistently lower than the C_{global} estimates, and this difference increased with increasing modeled prey abundance (Figure 5). At the highest modeled prey abundance (n = 900 individuals), the difference in C_{global} and the median of C_{local} ranged from 3.3–6.8 J timestep^{-1} predator^{-1}. The variance in the C_{local} confidence interval increased with increasing modeled prey abundance, ranging from 0.2–15.2 J timestep^{-1} predator^{-1} (Figure 5). These calculations consider the potential individual consumption rate with an assumed 70% predation success rate. The differences in C_{global} and C_{local} as well as differences among predator individuals is anticipated to accumulate with more individuals and become more variable in more complex models.

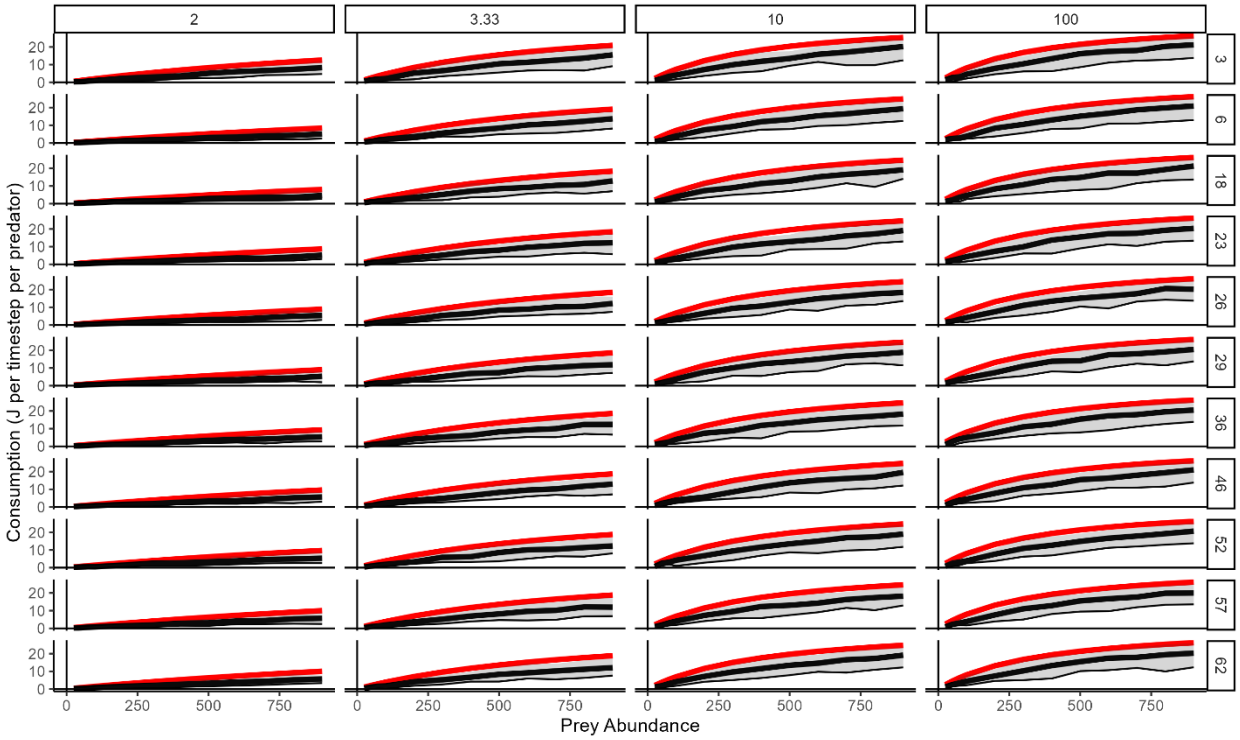

Figure 5. The consumption rates derived as a function of prey density encounter rates as a function of prey abundance. Relationships are divided among all relative swimming velocity (columns) and prey visual ranges greater than 0 m (rows) that followed a Type II response curve. Both grid-based response curves (red line) and individual-based response curves (gray ribbon) are shown. The black line corresponds to the median of the

Discussion

Predator-prey encounter rates are primarily influenced by prey density and, in this simplistic ecosystem, lead to the emergence of a Type II ecological functional curve when the predator is faster than the prey. The inclusion of prey behavior through varying swimming velocities, visual ranges, and an optimal prey movement algorithm shows that individual animal behavioral decisions affect these functional response curves. The trophic level of carnivorous fishes scales positively with body size (Keppeler et al. 2020) and many open-ocean species follow size-selective feeding patterns (Menard et al. 2006, Van Den Hoff et al. 2018). Although there is evidence for taxon-specific feeding within prey communities (Spitz et al. 2010, Drazen and Sutton 2017), morphological constraints (e.g., gape size) mean mobile predators generally feed

upon preys smaller than themselves. Similarly, marine predators are often faster than prey because of the physical advantage of being a larger object moving through a liquid medium (Domenici 2001). In this study, there was a dramatic decline in encounter rate estimates between the swimming velocity ratios 10:1 (i.e., predator is 10x faster than prey) – 1:1 (predator and prey have equal velocities), and little difference between ratios of 100:1–10:1 and 1:1–1:10. Therefore, there is a limitation to this influence on encounter rates, where predators that are currently 10x faster than their prey would not benefit from becoming faster, and *vice versa*. Additionally, the effect of relative swimming speed on encounter rates grows with increasing prey abundances until the prey abundance at which the functional response curve reaches an asymptote. In reality, animals are not constantly moving at their cruising or burst velocities, and it is likely they accelerate or decelerate between the two according to a gaussian function, with turbulence also affecting the acceleration of small organisms (Rothschild and Osborn 1988, Evans 1989). Considering that predator and prey would likely have offsetting cruise and burst velocities, as well as reaction times to recognize the other individual's movement, the inclusion of dynamic swimming velocities would likely add to the encounter rate variance quantified in this study. Prey behavior is capable of modulating encounter rates in marine ecosystems, and this should be considered when utilizing equations to model encounter rates in individual-based assessments.

The effect of relative swimming velocity on predator-prey encounter rates was enhanced when preys could perceive their environment and make informed movement decisions, rather than moving at a random vector. The visual acuity of marine fishes is related to eye size, which varies widely in the open-ocean realm (Caves et al. 2017). However, increasing the prey visual range beyond three meters had a negligible impact on the functional response curve, suggesting

306 visual range for the purposes at predator avoidance is only relevant at small scales. In a more
307 complex simulation where animals have multiple motivations (e.g., three or more species,
308 multiple predator or prey species, considerations to environmental and distance-based energetic
309 constraints), enhanced visual capabilities may have a greater influence on predator avoidance
310 success, as individuals would have to prioritize their optimal movement strategies.

311 Cooperative foraging strategies are used by many marine predators to increase the predation
312 efficiency of individual predators (Heithaus and Dill 2009, Hansen et al. 2022). This tactic was
313 not explicitly incorporated into this model, but all predators did have a shared motivation
314 (catching the nearest prey). Encounter rates should have been absent in scenarios with a prey
315 swimming speed greater than the predator, optimal movements, and no boundary effects that
316 could trap preys. Instead, multiple predators with an independent, shared motivation eventually
317 left a small number of preys with no optimal location away from the nearest predator. Individual-
318 based models that incorporate motivated animal movements do not need to make *a priori*
319 assumptions about cooperative foraging behaviors, as they will emerge as an aggregated result of
320 the decision-making process of each individual.

321 An emergent feature of this individual-based framework was patchiness of preys created
322 through random placements of individuals and consistent prey movements away from predators.
323 The energetic trade-offs associated with patchy prey environments influence optimal predator
324 movements and survivability (Zollner and Lima 2005). This leads to predators being distributed
325 according to an Ideal Free Distribution, a learned behavior where an individual predator is most
326 likely to situate itself near a patch that maximizes its prey encounter rates (Fretwell and Lucas
327 1970, Kacelnik et al. 1992). High prey abundances lead to increased variance in this patchiness
328 effect, meaning that the local prey density and variance among individual predators is dynamic

with changes to prey abundance, a factor that could only be explored when explicitly modeling individual predator efficiencies. Moreover, the difference in globally and locally derived consumption estimates is an example of Jensen's inequality, a statistical concept where the expected value from a convex (non-linear) function is greater than or equal to the expected value from an individual sample (McShane 1937). Since predators are able to associate with prey patches (Benoit-Bird et al. 2013) and these patches have an effect on individual consumption rates, we argue that local prey density is more accurate estimation than global prey density and should be utilized in advanced food-web modeling efforts.

Acknowledgements

This concept originated from a JuliaOcean workshop led by XX and XX. MW is supported by a WHOI Postdoctoral Scholarship (may not need this).

Data Availability

The Julia code for these simulations is available in a public GitHub repository (https://github.com/fishesofthedeep/EncounterRates) and available upon request by the authors. All input parameters for the model are listed in the Methods section and embedded within the model code.

Literature Cited

Anderson, T. W. 2001. Predator responses, prey refuges, and density-dependent mortality of a marine fish. Ecology 82:245–257.

Banville, F., S. Vissault, and T. Poisot. 2021. Mangal.jl and EcologicalNetworks.jl: Two complementary packages for analyzing ecological networks in Julia. The Journal of Open Source Software 6:2721.

Benoit-Bird, K. J., B. C. Battaile, S. A. Heppell, B. Hoover, D. Irons, N. Jones, K. J. Kuletz, C. A. Nordstrom, R. Paredes, R. M. Suryan, C. M. Waluk, and A. W. Trites. 2013. Prey Patch Patterns Predict Habitat Use by Top Marine Predators with Diverse Foraging Strategies. PLOS ONE 8:e53348.

Caves, E. M., T. T. Sutton, and S. Johnsen. 2017. Visual acuity in ray-finned fishes correlates with eye size and habitat. Journal of Experimental Biology 220:1586–1596.

Chan, K., S. Boutin, T. Hossie, C. Krebs, M. O'Donoghue, and D. Murray. 2017. Improving the assessment of predator functional responses by considering alternate prey and predator interactions. Ecology 98:1787–1796.

Cosner, C., D. DeAngelis, J. Ault, and D. Olson. 1999. Effects of Spatial Grouping on the Functional Response of Predators. Theoretical Population Biology 56:65–75.

Domenici, P. 2001. The scaling of locomotor performance in predator–prey encounters: from fish to killer whales. Comparative Biochemistry and Physiology Part A: Molecular & Integrative Physiology 131:169–182.

Drazen, J. C., and T. T. Sutton. 2017. Dining in the deep: the feeding ecology of deep-Sea fishes. Annual Review of Marine Science 9:337–366.

Evans, G. T. 1989. The encounter speed of moving predator and prey. Journal of Plankton Research 11:415–417.

Fretwell, S., and H. Lucas. 1970. On territorial behaviour and other factors influencing habitat distribution in birds. I. Theoretical development. Acta Biotheor 19:16–36.

Grabowski, J. H. 2004. Habitat complexity disrupts predator–prey interactions but not the trophic cascade on oyster reefs. Ecology 85:995–1004.

Hansen, M. J., S. Krause, F. Dhellemmes, K. Pacher, R. H. J. M. Kurvers, P. Domenici, and J. Krause. 2022. Mechanisms of prey division in striped marlin, a marine group hunting predator. Communications Biology 5:1161.

Heithaus, M. R., and L. M. Dill. 2009. Feeding strategies and tactics. Pages 414–423 Encyclopedia of marine mammals. Elsevier.

Jeschke, J., M. Kopp, and R. Tollrian. 2002. Predator Functional Responses: Discriminating Between Handling and Digesting Prey. Ecological Monographs 72:95–112.

Kacelnik, A., J. R. Krebs, and C. Bernstein. 1992. The ideal free distribution and predator-prey populations. Trends in Ecology & Evolution 7:50–55.

Keppeler, F. W., C. G. Montaña, and K. O. Winemiller. 2020. The relationship between trophic level and body size in fishes depends on functional traits. Ecological Monographs 90:e01415.

Kratina, P., M. Vos, A. Bateman, and B. Anholt. 2009. Functional responses modified by predator density. Oecologia 159:425–433.

Levin, S. 1994. Patchiness in marine and terrestrial systems: from individuals to population. Philosophical Transactions: Biological Sciences 343:99–103.

Li, Y., B. Rall, and G. Kalinkat. 2018. Experimental duration and predator satiation levels systematically affect functional response parameters. Oikos 127:590–598.

Liao, J. 2007. A review of fish swimming mechanics and behaviour in altered flows. Philosophical Transactions of the Royal Society B 362:1973–1993.

Mattila, J., K. L. Heck Jr, E. Millstein, E. Miller, C. Gustafsson, S. Williams, and D. Byron. 2008. Increased habitat structure does not always provide increased refuge from predation. Marine Ecology Progress Series 361:15–20.

McShane, E. J. 1937. Jensen's inequality.

Menard, F., C. Labrune, Y.-J. Shin, A.-S. Asine, and F.-X. Bard. 2006. Opportunistic predation in tuna: a size-based approach. Marine Ecology Progress Series 323:223–231.

Papanikolaou, N. E., G. D. Broufas, D. P. Papachristos, M. L. Pappas, C. Kyriakaki, K. Samaras, and T. Kypraios. 2020. On the mechanistic understanding of predator feeding behavior using the functional response concept. Ecosphere 11:e03147.

Papastamatiou, Y. P., B. M. Binder, K. M. Boswell, M. A. Malone, M. R. Heithaus, C. Huveneers, J. Mourier, and A. R. Harborne. 2023. Dynamic energy landscapes of predators and the implications for modifying prey risk. Functional Ecology.

Plagányi, É. E., A. E. Punt, R. Hillary, E. B. Morello, O. Thébaud, T. Hutton, R. D. Pillans, J. T. Thorson, E. A. Fulton, A. D. M. Smith, F. Smith, P. Bayliss, M. Haywood, V. Lyne, and P. C. Rothlisberg. 2014. Multispecies fisheries management and conservation: Tactical applications using models of intermediate complexity. Fish and Fisheries 15:1–22.

Preisser, E. L., D. I. Bolnick, and M. F. Benard. 2005. Scared to death? The effects of intimidation and consumption in predator–prey interactions. Ecology 86:501–509.

R Core Team. 2023. R: A Language and Environment for Statistical Computing. R Foundation for Statistical Computing, Vienna, Austria.

Rothschild, B. J., and T. R. Osborn. 1988. Small-scale turbulence and plankton contact rates. Journal of Plankton Research 10:465–474.

Spitz, J., E. Mourocq, J.-P. Leauté, J.-C. Quéro, and V. Ridoux. 2010. Prey selection by the common dolphin: Fulfilling high energy requirements with high quality food. Journal of Experimental Marine Biology and Ecology 390:73–77.

Thiele, J., W. Kurth, and V. Grimm. 2011. . Pages 68–101 *in* K. Römisch, A. Nothdurft, and U. Wunn, editors. Agent- and Individual-based Modeling with NetLogo: Introduction and new NetLogo Extensions. Die Grüne Reihe 22. Tagung der Sektion Forstliche Biometrie und Informatik des Deutschen Verbandes Forstlicher Forschungsanstalten und der

Arbeitsgemeinschaft Ökologie und Umwelt der Internationalen Biometrischen Gesellschaft, Göttingen (Germany).

Van Den Hoff, J., C. Eriksson, H. Burton, and M. Schultz. 2018. Size-Selective Feeding by Mesopelagic Fish Can Impact Ocean Surface Abundance of Small Plastic Particles.

Wu, Z., and G. Forget. 2022. PlanktonIndividuals. jl: a GPU supported individual-based phytoplankton life cycle model. Journal of Open Source Software 7:4207.

Zollner, P. A., and S. L. Lima. 2005. Behavioral tradeoffs when dispersing across a patchy landscape. Oikos 108:219–230.

Supplementary Material

The following plots are all renditions of Figure 4A at different prey swimming velocities (panels) and visual ranges (full figures ordered smallest visual area to largest)

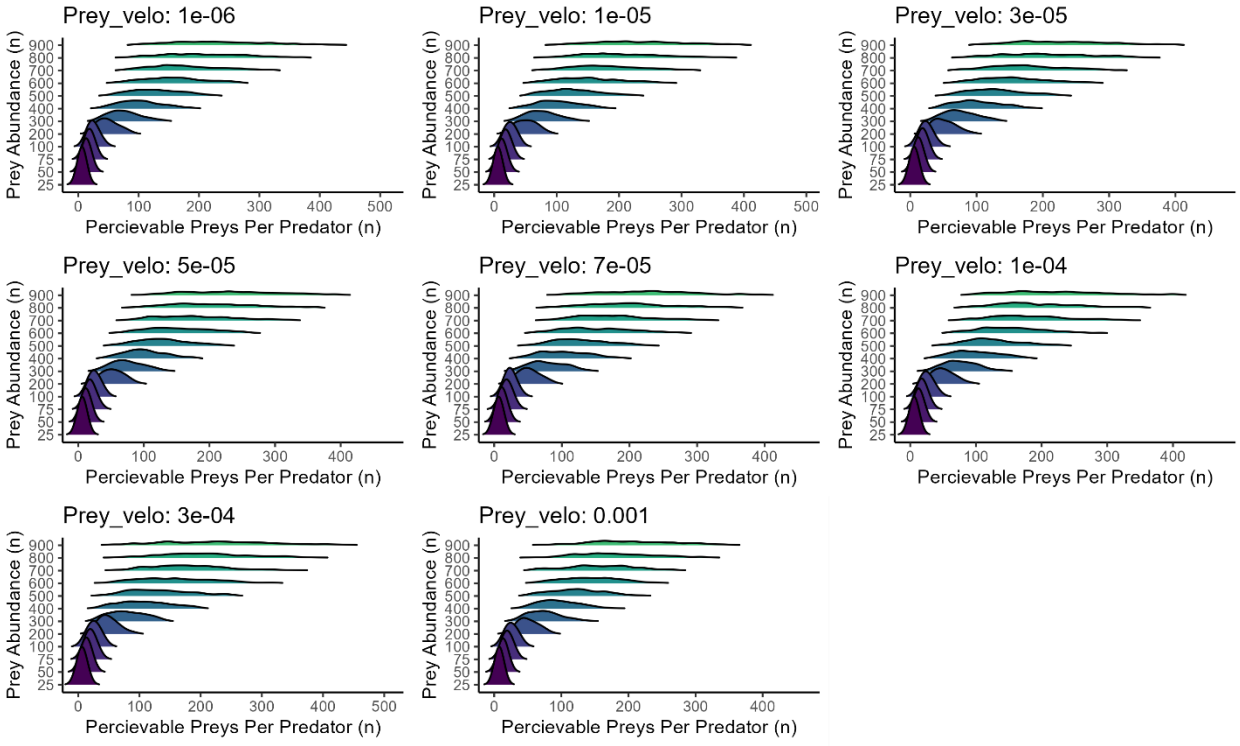
Prey_velo: 1e-06
Prey_velo: 1e-05
Prey_velo: 3e-05
Prey_velo: 5e-05
Prey_velo: 7e-05
Prey_velo: 1e-04
Prey_velo: 3e-04
Prey_velo: 0.001
Prey Abundance (n)
Percievable Preys Per Predator (n)

433

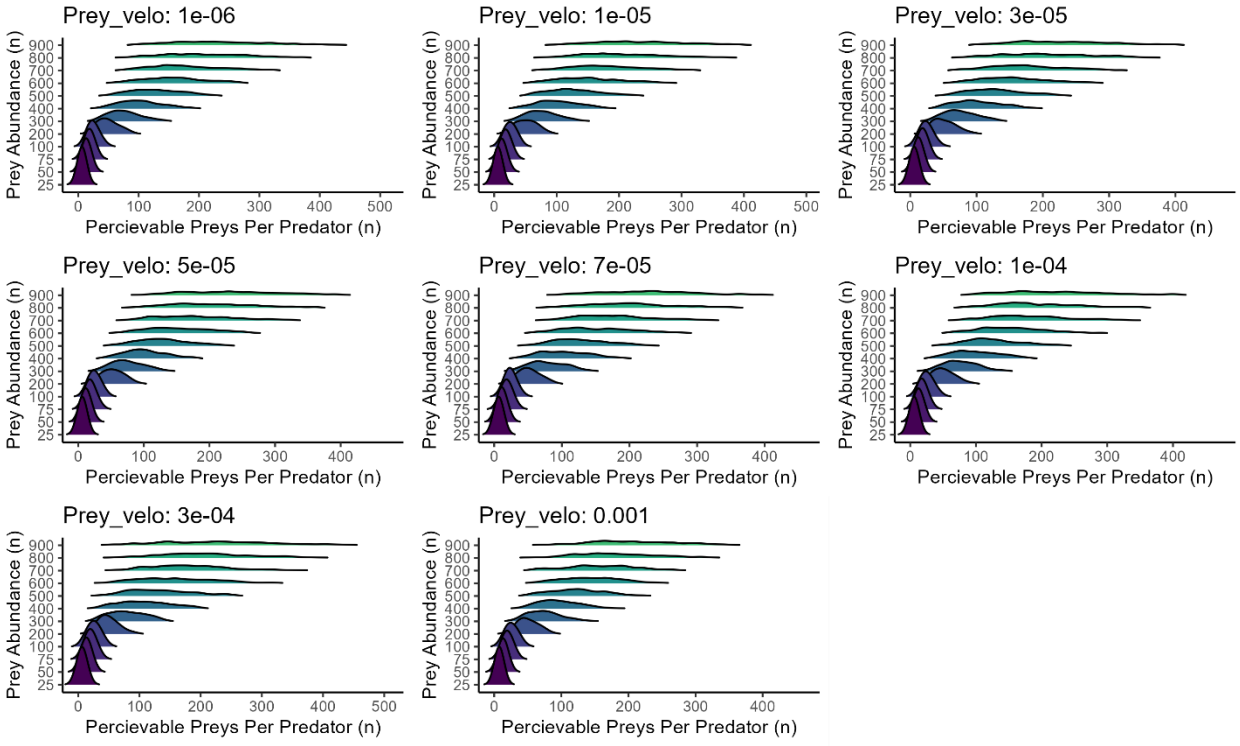
Prey_velo: 1e-06
Prey_velo: 1e-05
Prey_velo: 3e-05
Prey_velo: 5e-05
Prey_velo: 7e-05
Prey_velo: 1e-04
Prey_velo: 3e-04
Prey_velo: 0.001
Prey Abundance (n)
Percievable Preys Per Predator (n)

434

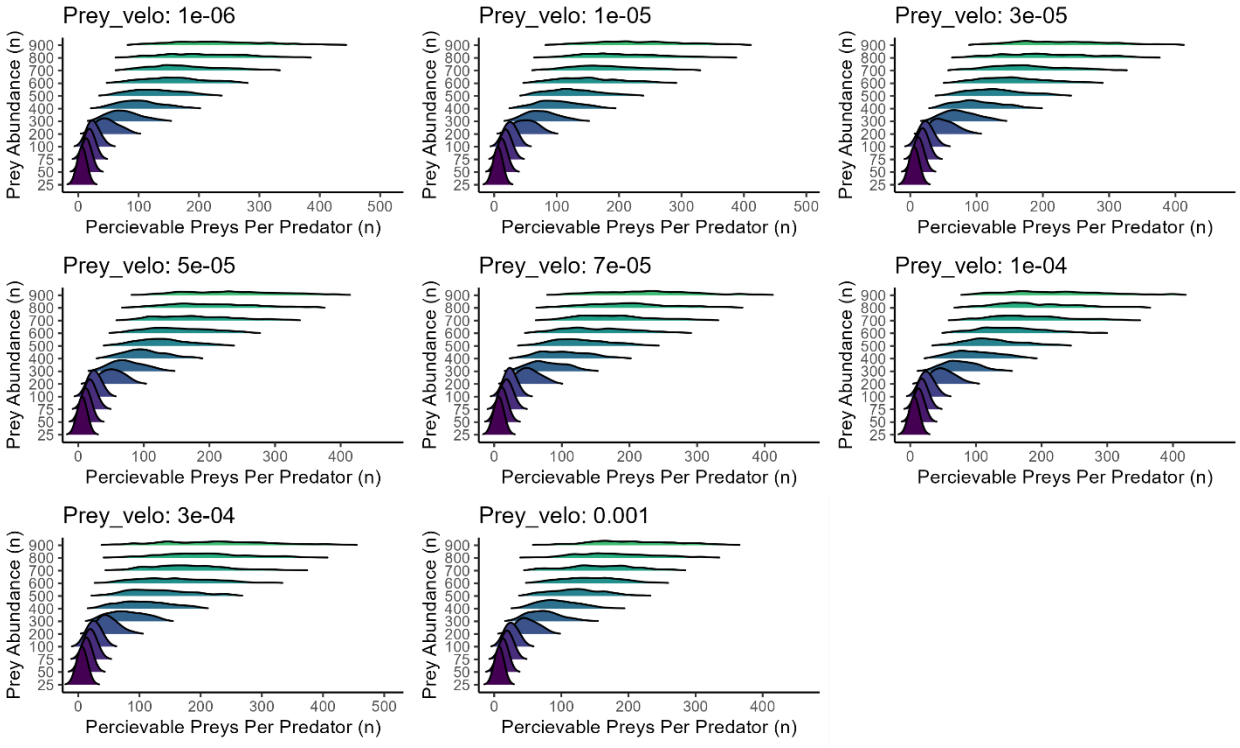
Prey_velo: 1e-06
Prey_velo: 1e-05
Prey_velo: 3e-05
Prey_velo: 5e-05
Prey_velo: 7e-05
Prey_velo: 1e-04
Prey_velo: 3e-04
Prey_velo: 0.001
Prey Abundance (n)
Percievable Preys Per Predator (n)

435

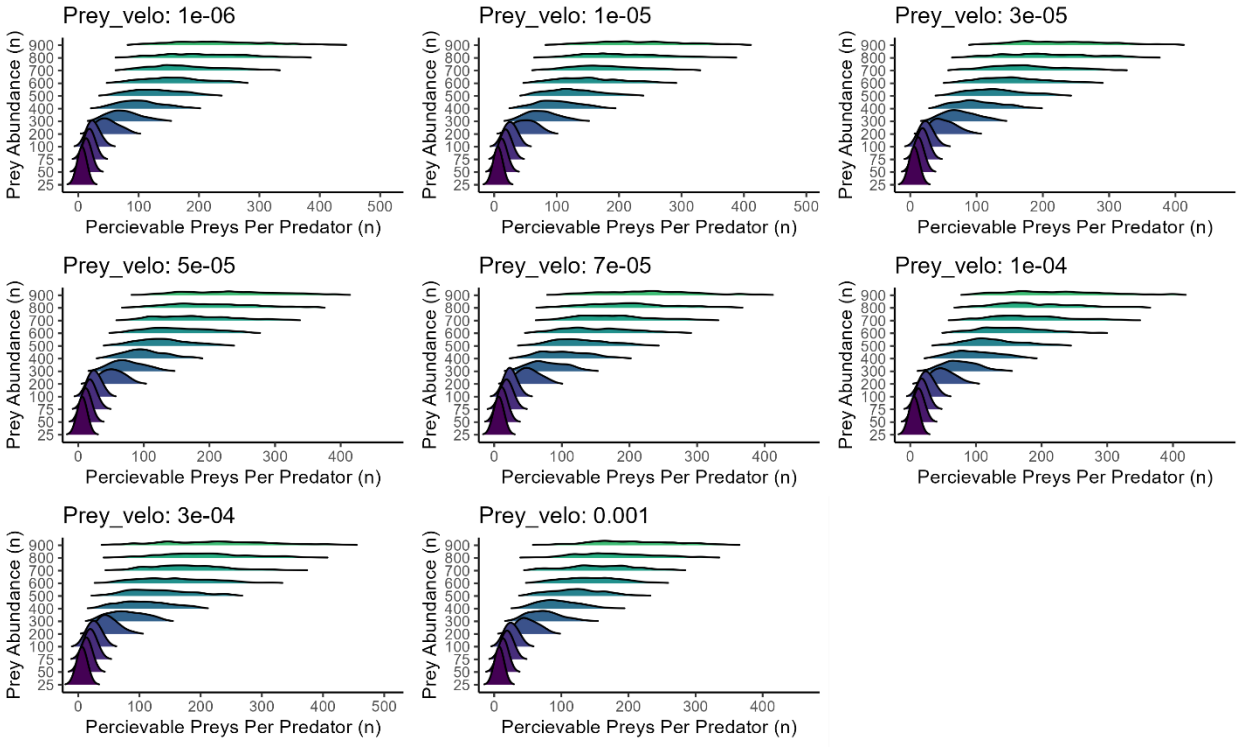
Prey_velo: 1e-06
Prey_velo: 1e-05
Prey_velo: 3e-05
Prey_velo: 5e-05
Prey_velo: 7e-05
Prey_velo: 1e-04
Prey_velo: 3e-04
Prey_velo: 0.001
Prey Abundance (n)
Percievable Preys Per Predator (n)

436

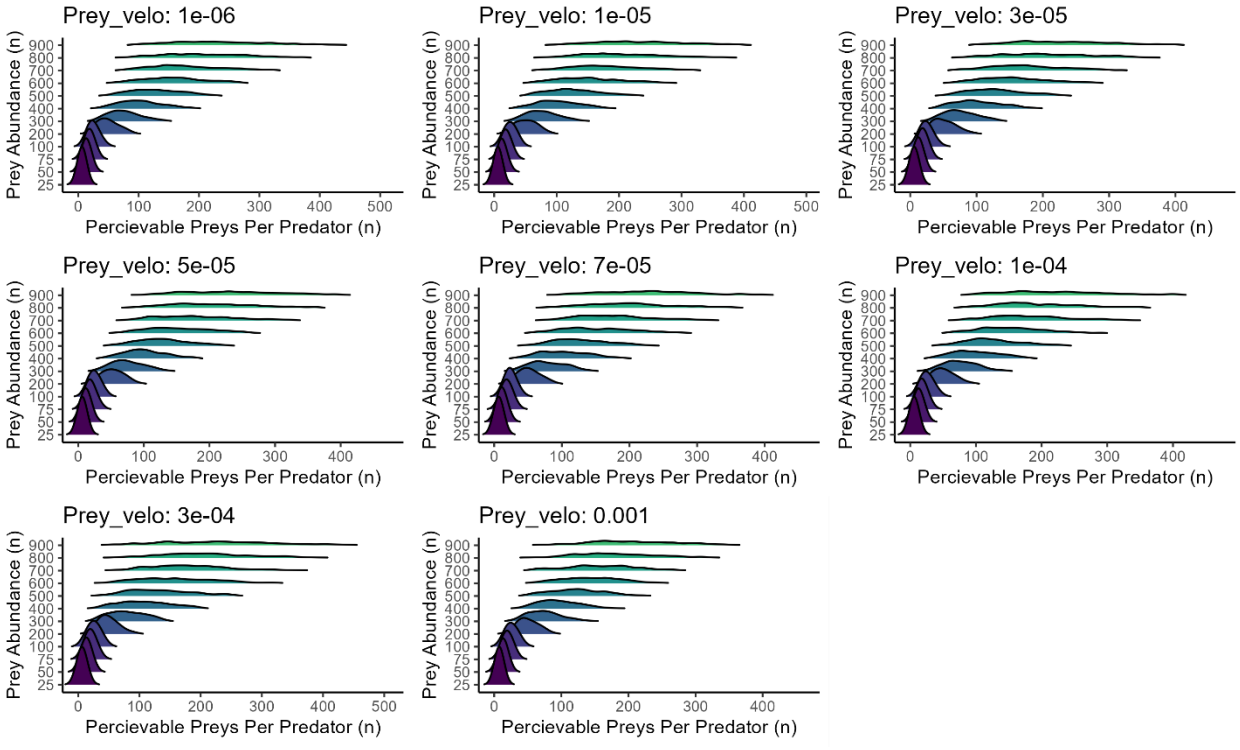
Prey_velo: 1e-06
Prey_velo: 1e-05
Prey_velo: 3e-05
Prey_velo: 5e-05
Prey_velo: 7e-05
Prey_velo: 1e-04
Prey_velo: 3e-04
Prey_velo: 0.001
Prey Abundance (n)
Percievable Preys Per Predator (n)

437

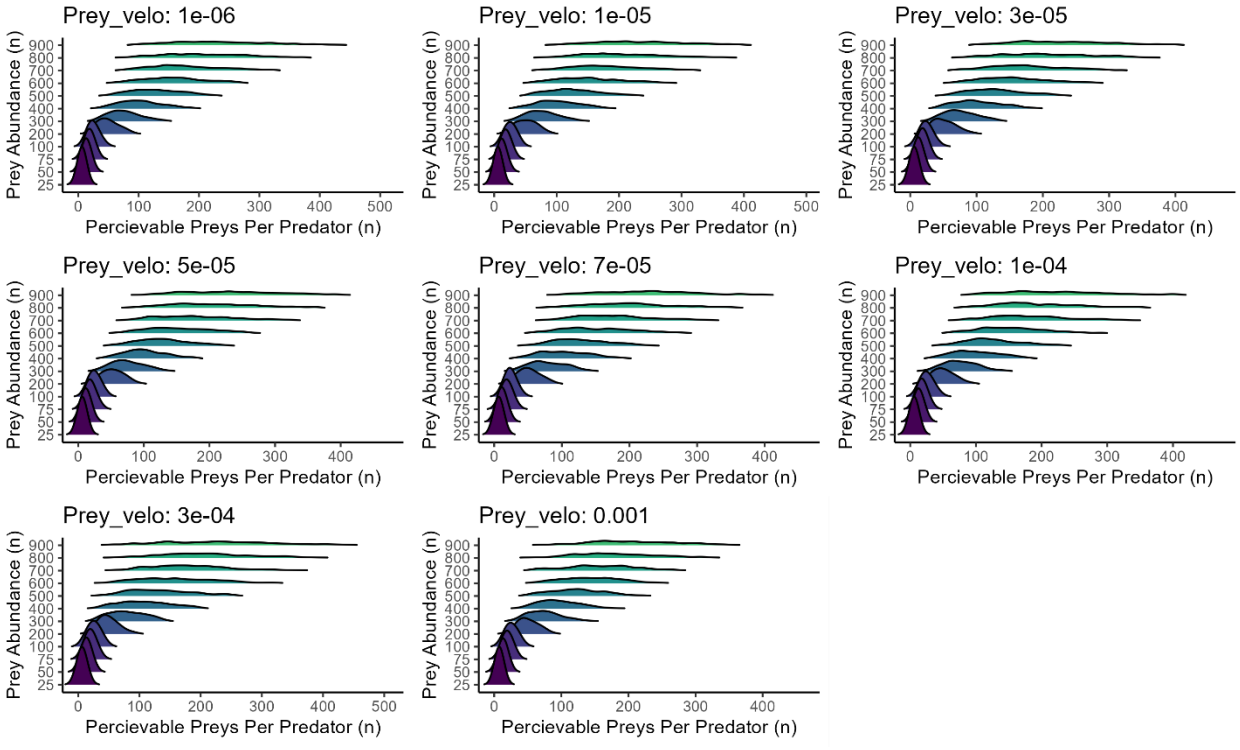
Prey_velo: 1e-06
Prey_velo: 1e-05
Prey_velo: 3e-05
Prey_velo: 5e-05
Prey_velo: 7e-05
Prey_velo: 1e-04
Prey_velo: 3e-04
Prey_velo: 0.001
Prey Abundance (n)
Percievable Preys Per Predator (n)

438

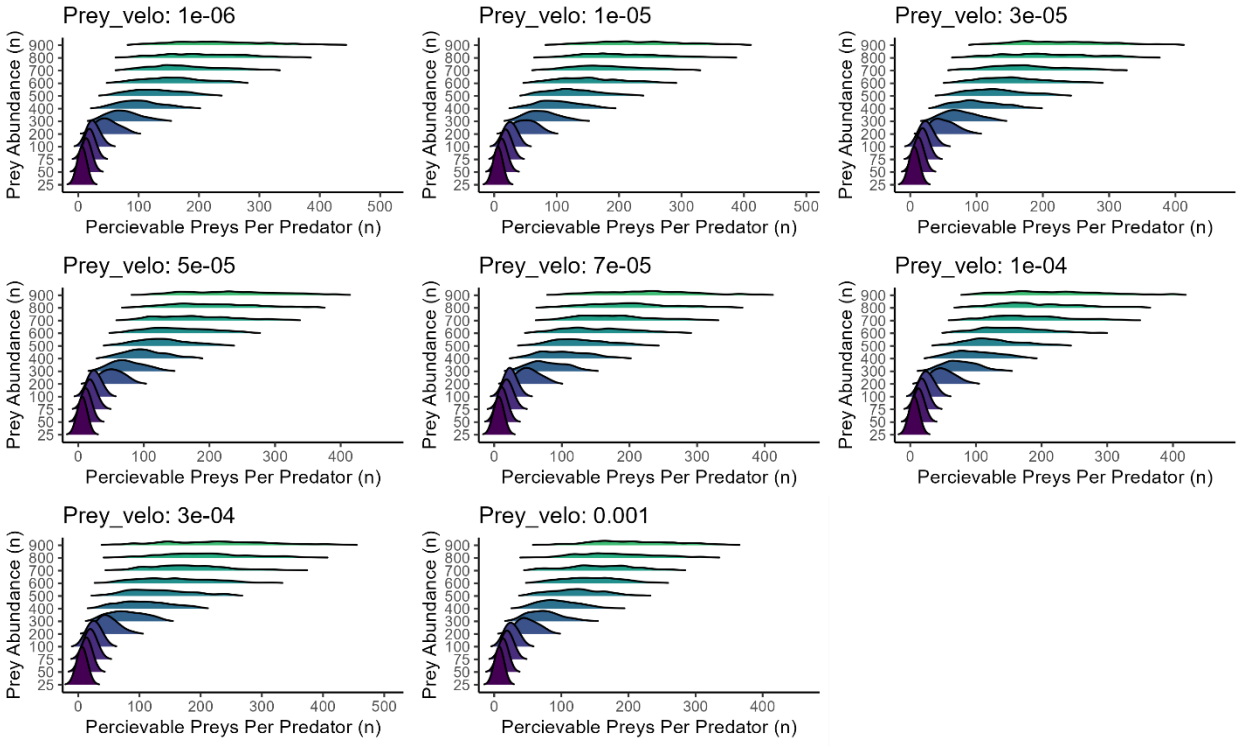
Prey_velo: 1e-06
Prey_velo: 1e-05
Prey_velo: 3e-05
Prey_velo: 5e-05
Prey_velo: 7e-05
Prey_velo: 1e-04
Prey_velo: 3e-04
Prey_velo: 0.001
Prey Abundance (n)
Percievable Preys Per Predator (n)

439

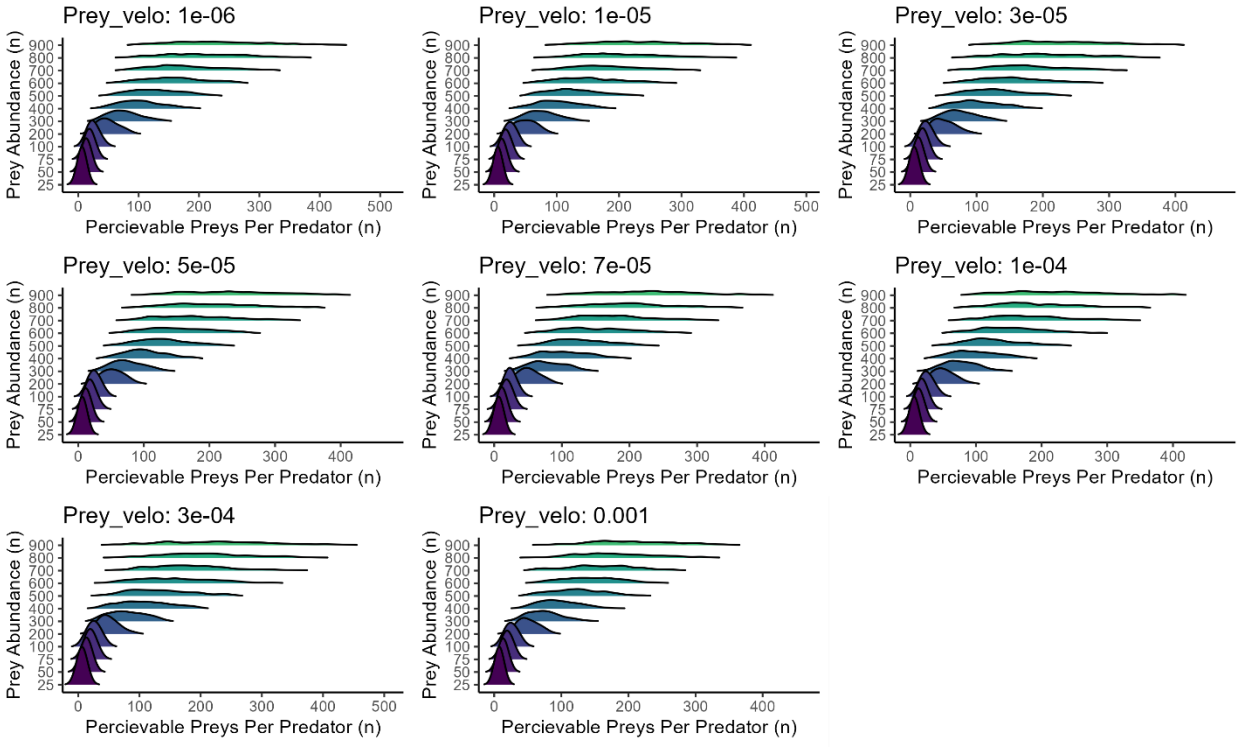
Prey_velo: 1e-06
Prey_velo: 1e-05
Prey_velo: 3e-05
Prey_velo: 5e-05
Prey_velo: 7e-05
Prey_velo: 1e-04
Prey_velo: 3e-04
Prey_velo: 0.001
Prey Abundance (n)
Percievable Preys Per Predator (n)

440

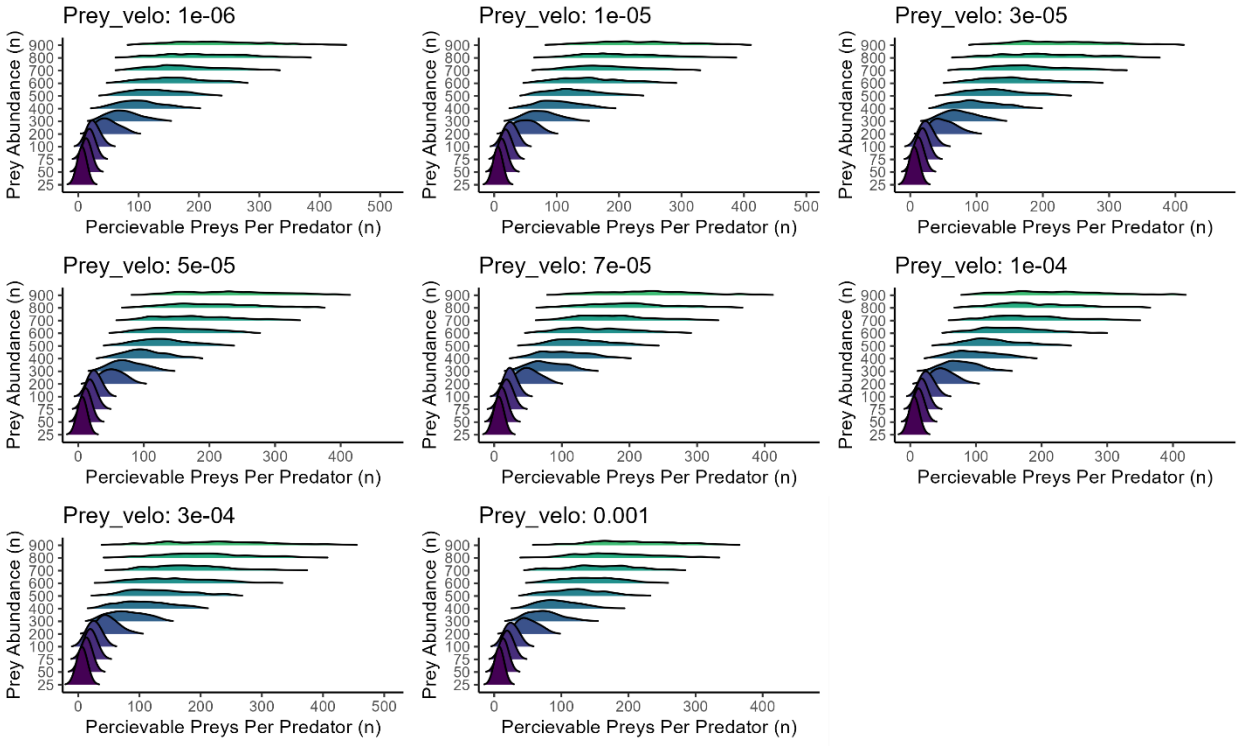
Prey_velo: 1e-06
Prey_velo: 1e-05
Prey_velo: 3e-05
Prey_velo: 5e-05
Prey_velo: 7e-05
Prey_velo: 1e-04
Prey_velo: 3e-04
Prey_velo: 0.001
Prey Abundance (n)
Percievable Preys Per Predator (n)

441

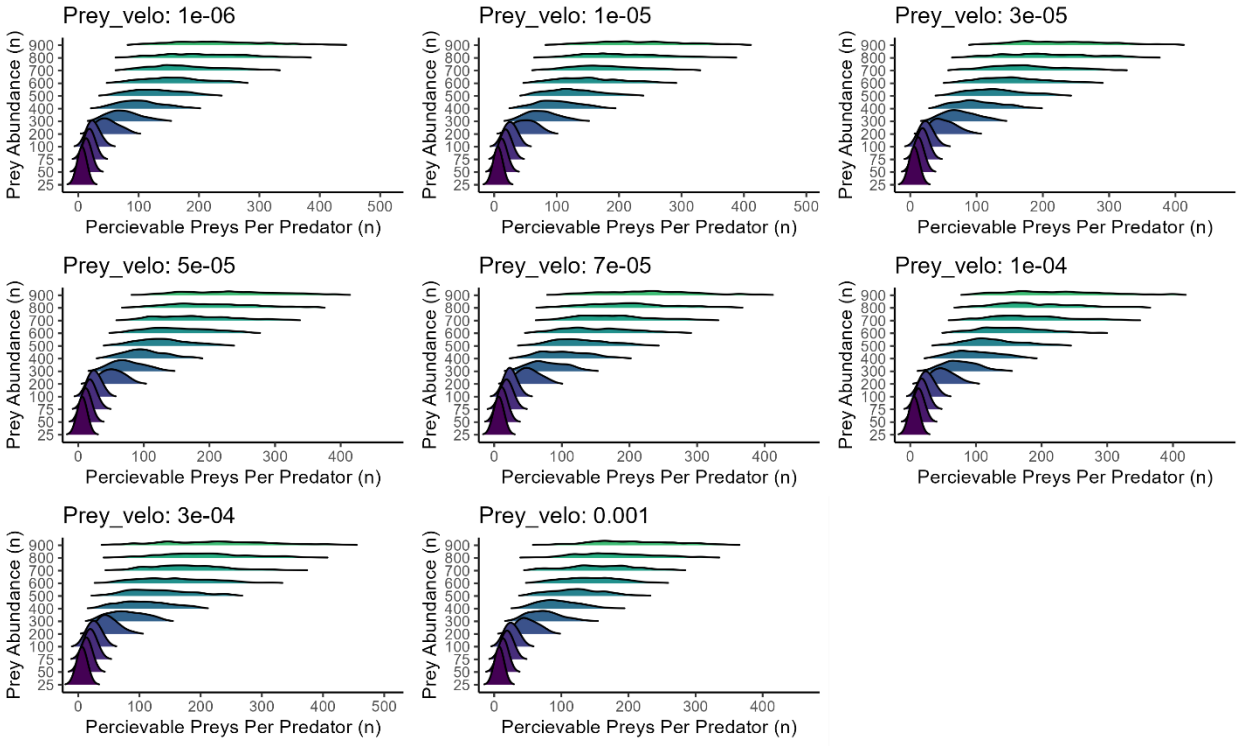
Prey_velo: 1e-06
Prey_velo: 1e-05
Prey_velo: 3e-05
Prey_velo: 5e-05
Prey_velo: 7e-05
Prey_velo: 1e-04
Prey_velo: 3e-04
Prey_velo: 0.001
Prey Abundance (n)
Percievable Preys Per Predator (n)

442

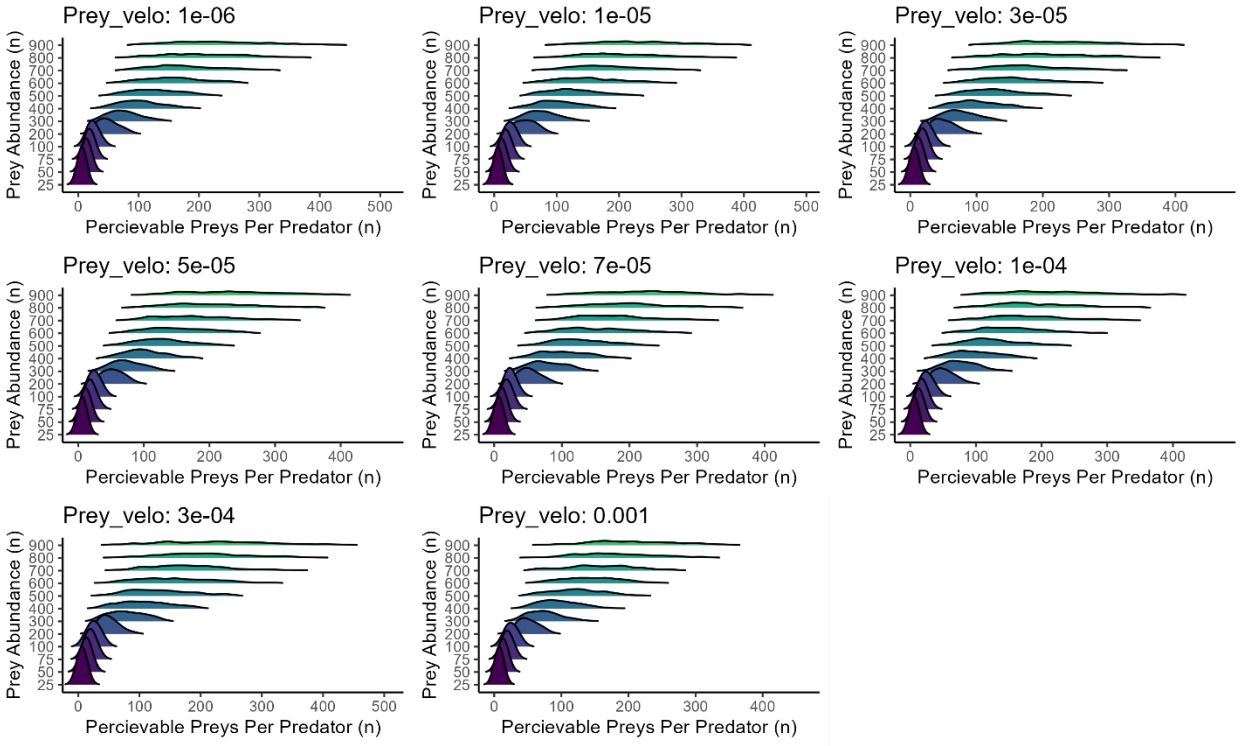
Prey_velo: 1e-06
Prey_velo: 1e-05
Prey_velo: 3e-05
Prey_velo: 5e-05
Prey_velo: 7e-05
Prey_velo: 1e-04
Prey_velo: 3e-04
Prey_velo: 0.001
Prey Abundance (n)
Percievable Preys Per Predator (n)

443

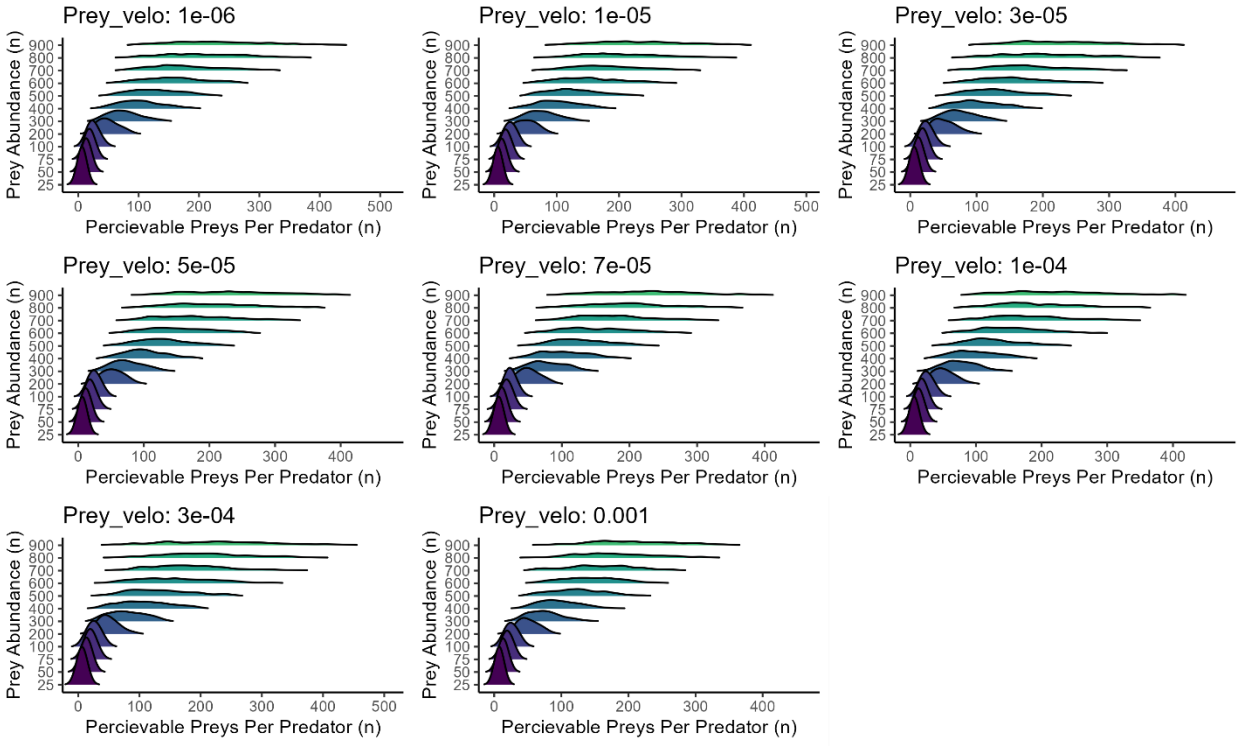
Prey_velo: 1e-06
Prey_velo: 1e-05
Prey_velo: 3e-05
Prey_velo: 5e-05
Prey_velo: 7e-05
Prey_velo: 1e-04
Prey_velo: 3e-04
Prey_velo: 0.001
Prey Abundance (n)
Percievable Preys Per Predator (n)

444

445